Environ Res Tec, Vol. 7, Issue. 1, pp. 108–117, March 2024

Environmental Research and Technology
https://ert.yildiz.edu.tr - https://dergipark.org.tr/tr/pub/ert
DOI: https://10.35208/ert.1306840

Research Article

Effect of purification methods on the quality and morphology of plastic waste-derived carbon nanotubes

Helen MODEKWE*, Ishmael RAMATSA

Renewable Energy and Biomass Research Group, Department of Chemical Engineering, Faculty of Engineering and the Built Environment, University of Johannesburg, South Africa

ARTICLE INFO

Article history
Received: 30 May 2023
Revised: 07 January 2024
Accepted: 13 January 2024

Key words:
Plastic waste derived carbon nanotubes; Purification methods; Chemical oxidation; Air oxidation; Morphology; Quality

ABSTRACT

Recent innovative research efforts on the usage of plastic wastes as a cheap carbon source for carbon nanotubes (CNTs) production have emerged as a low-cost and sustainable means of producing CNTs. However, plastic waste-derived CNTs are rarely used in some purity-sensitive and high-alignment needed applications due to the poor quality of CNTs resulting from the abundance of impurities such as non-crystalline amorphous carbon, metallic nanoparticles, and other impurities. Therefore, purification is a crucial issue to be addressed to fully harness all potential applications of CNTs derived from waste plastic materials. Here, the effect of employing different purification methods on the morphology and purity of waste plastic-derived CNTs was investigated. CNTs were synthesized using waste polypropylene plastic as carbon feedstock via a single-stage catalytic chemical vapour deposition (CVD) technique. As-produced CNTs were purified using liquid-phase oxidation (chemical oxidation in nitric acid), gas-phase oxidation in air, and a combination of both liquid- and gas-phase oxidation methods. The synthesized and purified CNTs were characterized for morphology, purity, surface functional groups, thermal stability, and crystallinity using Transmission electron microscopy (TEM), Raman spectroscopy, Fourier Transform Infrared spectroscopy (FTIR), Thermogravimetric analysis (TGA), and X-ray diffraction (XRD), respectively. Results obtained showed that a combination of both liquid and gas phase oxidation purification techniques resulted in purer, better quality, and less defective CNTs with an IG'/IG value of 0.89 and ID/IG value of 0.86, while chemically treated CNTs (CNT-PC) presented more structurally defective CNTs and shortened nanotubes compared to other investigated treatment methods with an ID/IG value of 0.96. CNTs purified by a multi-step protocol (CNT-PAC) showed the highest weight loss of 72.3% indicating the highest quality and the presence of filamentous carbon. This study confirms that the choice of purification techniques influences the morphology and quality of plastic-derived CNTs.

Cite this article as: Modekwe H, Ramatsa I. Effect of purification methods on the quality and morphology of plastic waste-derived carbon nanotubes. Environ Res Tec 2024;7(1)108–117.

INTRODUCTION

Carbon nanotubes (CNTs) are a one-dimensional (1D) allotropic form of carbon whose diameter exists in the nanometer and its length in micrometer scale [1, 2]. CNTs consist of mainly three types namely: single-walled (SWCNTs), double-walled (DWCNTs), and multi-walled (MWCNTs). These materials possess extraordinary physicochemical properties, including high mechanical strength, excellent optical, thermal stability, and electrical conductivity properties, as well as large surface area, high aspect ratio, etc. The versatile potential applications of CNTs as functional

---

***Corresponding author.**
*E-mail address: uche_lyne2@yahoo.com

Published by Yıldız Technical University Press, İstanbul, Türkiye

materials in various fields of science, engineering, medicine, manufacturing, electronics, construction, etc. [3] have accelerated the global CNTs production capacity from 400–460 tons in 2013 [4] and are forecasted to reach 7000 tons by 2025 [5]. In 2019, the global CNTs market value was about $670.5 million, with a compound annual growth rate (CAGR) of about 34% [6, 7]. Some of the existing applications of CNTs are in hydrogen storage, reinforcement materials in high-strength composites and polymers, drug delivery and tissue engineering, water purification, CO_2 capture and storage, energy storage and conversion, catalysis, sensors, etc. [1, 2]. In 2019, CNTs accounted for the highest market share of 26.9% in energy-related nanomaterials [8].

The different methods used in the synthesis of CNTs are laser ablation, chemical vapour deposition, and electric-arc discharge [1]. Depending on the method of CNTs' production, CNTs are usually prepared using carbonaceous materials as the sources of carbon and in the presence of heat. In addition, metallic catalysts are usually incorporated during the synthesis process to improve the product yield and also catalyze the breakdown of hydrocarbon molecules, thereby reducing the temperature gradient and the reaction rate, which impact the energy requirement and cost (by indirectly reducing the cost of production) [9]. Depending on the synthesis technique employed, the nanotube powder produced contains a considerable number of other impurities, ranging from residual unreacted metal catalysts, amorphous carbon, nanocrystalline graphite, fullerenes, and other unwanted materials. The presence of these impurities reduces CNTs' performance and potential applications in various fields [10, 11].

Also, heterogenous catalysts used in CNTs growth are embedded in various metal oxides as catalyst supports to achieve desired active metal stability, improve active metal dispersion, minimize agglomeration, and assist in obtaining good and small active metal particle sizes [12]. These supports are very hard to remove, and using certain harsh purification treatment methods destroys the structural integrity of the nanotubes and restricts their performance in certain real-life applications [13].

The production and consumption of plastic materials have continued to increase over the years due to the increasing population as well as high demand from household and industrial applications [14]. In 2018, global plastic production reached 360 million tonnes [15]. According to the report by Geyer et al. [16], as little as 9% of the global plastic waste is recycled, 19% is incinerated, and 22% of this generated waste is mismanaged and unaccounted for, while a larger percentage (50%) of generated plastic wastes is discarded in landfills [16]. Plastics account for over 75% of the total marine litter [17], and it was estimated in 2010 that about 4.8–12.7 million metric tonnes of plastic entering the ocean each year are mostly from land-based sources [17].

Waste plastics are composed of very high carbon content; the use of plastic wastes as cheap feedstock in the synthesis of CNTs has the potential to replace the commonly used high-purity light-weight hydrocarbon materials such as methane, acetylene, benzene, etc., which have other important industrial uses. However, due to the complex nature of plastics, utilizing them as feedstock in CNTs production results in the formation of more complicated and complex structures and unreacted carbon together with other nanomaterials (such as fullerenes, nanofibers, nano-onions, graphite, nanosheets, and so on). Therefore, apart from the usual unreacted metal catalysts, enormous quantities of amorphous carbons are expected as impurities and need to be removed from plastic waste-derived CNTs. Hence, choosing a particular treatment method that will remove all or considerable quantities of impurities present in plastic-derived CNTs without damaging the original length and structural integrity of CNTs is more of a difficult task.

The major purification methods are grouped into chemical and physical methods [18]. In using the chemical oxidation purification techniques, CNTs purification is based on the principle that metallic nanoparticles dissolve easily in acids or bases, while gas-phase oxidation treatment is also based on the fact that carbonaceous impurities oxidize at a faster rate than CNTs [19]. Purification by chemical treatment presents defects on the nanotubes' wall surface and results in a pentagonal structure on the nanotubes' ends, resulting in the loss of a considerable amount of CNTs with a deformed structure and morphology of the nanotubes [19].

Common oxidative treatment methods are gas-phase oxidation (using oxidants such as air, steam, etc. at an oxidation temperature range of 225 to 760 °C; this method is usually employed to remove molecules adsorbed inside the matrices of CNTs and oxidize thermally unstable non-crystalline carbon). A study by Boncel and Kozoil [20] utilized thermal treatment in argon for the removal of encapsulated iron metal in MWCNTs. Clancy et al. [21] conducted a comparison study on several purification routes (acid treatment (HNO_3, HCl, H_2O_2/HCl), gas-phase (air oxidation, water vapour), electrochemical reduction and reduction with NaNP/DMAc (using sodium naphthalide in dimethylacetamide) for purifying commercial SWCNTs type (Tuball™). According to their study, SWCNTs purification by air oxidation does not result in functionalization of the tubes, and amorphous carbon was significantly reduced, However, the technique was not efficient in metal catalyst removal.

Other oxidative treatment methods such as liquid-phase oxidation (which involves treatment with oxidizing agents and mineral acids such as $KMnO_4$, H_2O_2, HNO_3, H_2SO_4, or their mixtures) and electrochemical oxidation are also employed in the purification of CNTs [19]. Hammadi et al. [22] reported the purification of CNTs synthesized from liquified petroleum gas by flame fragment deposition using a 2-step process that involved sonicating the produced sample in a hydrogen peroxide solution and then ultrasonicating it in an acetone bath. Their TEM result indicated that some residual nanocapsules (carbon quantum dots) were unable to be removed using this H_2O/acetone method. Pelech et al. [23] have used two methods in the removal of metals from CNTs. The first step involves the use of acid reflux in nitric acid, and the second method in-

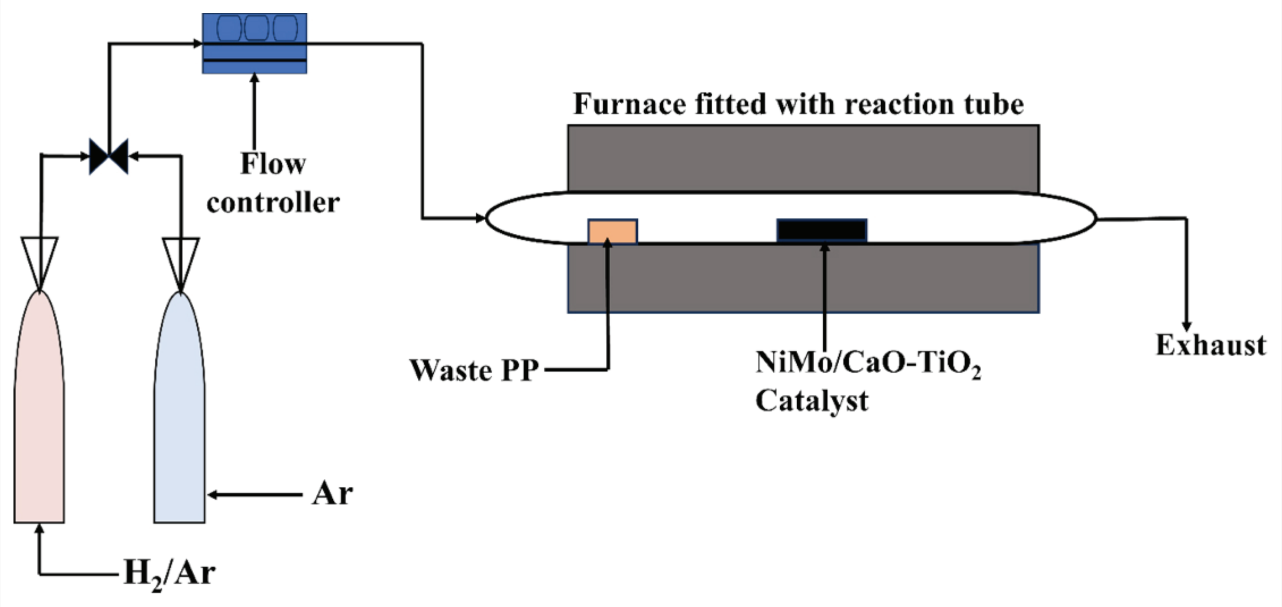

Figure 1. The schematic diagram for the production of CNTs from waste PP using the single-stage CVD technique.

volves microwave-assisted digestion. Their result suggested that microwave heating at elevated pressure improved the purification efficiency, and a similar removal degree was obtained using both acid reflux and microwave-assisted acid digestion techniques.

The physical method is usually used to remove impurities such as nanocapsules and amorphous carbon, or even in the separation of different length and diameter ratios of CNTs. Physical treatment based on ultrasonication, size-exclusion chromatography, filtration, and centrifugation involves the separation of unwanted materials based on variations in gravity, physical sizes, magnetic properties, aspect ratio, and so on [13, 18]. Although some of these physical treatment-based techniques are invariably applied in almost all CNTs' purification studies. A recent study examined the effect of purification on the electrical properties of SWCNTs produced by electric arc discharge using thermal air oxidation and acid oxidation. The reported result showed that purification not only impacted the electrical properties of SWCNTs but also affected the conductivity of SWCNTs, their length, and bundle diameter. Thermal air-oxidized SWCNTs had lower purity but higher conductivity compared to acid-treated SWCNTs [24].

Little or no study in the open literature has essentially evaluated the influence of the various purification protocols on the quality and structure of plastic waste-derived CNTs, despite the growing research interest in the use of plastic wastes as a source of carbon for CNTs synthesis. Plastic waste-derived CNTs have proven to be a sustainable means of eradicating waste and also a viable, cheap, and available hydrocarbon raw material for producing CNTs and other nanomaterials [25]. There is currently no ideal purification method for plastic waste-derived CNTs, as the various purification routes available in the open literature are applied to CNTs produced from different sources. Plastic-derived CNTs have a higher impurity density due to their inherent complex hydrocarbon nature. Therefore, this study aimed to investigate the effect of three different purification methods on the structural morphology and purity of polypropylene (PP) waste-derived CNTs. This approach is necessary to open up more research efforts towards expanding the possible applications of plastic (wastes)-derived CNTs in other fields of science.

MATERIALS AND METHODS

Materials

Already prepared catalyst: Ni-Mo/CaO-TiO$_2$ catalyst used in this work was obtained from a previous study [26]. Deionized water (DI water) and nitric acid (Sigma-Aldrich, South Africa, AR, 65% purity) were utilized in the purification process.

Synthesis of CNTs from PP Waste

The University of Johannesburg, Doornfontein campus's garbage deposit/pick-up point provided the waste PP material used (waste PP consisting of household food packaging was collected at the mentioned garbage point above). The obtained waste materials were then washed, dried, and broken into small bits using a jaw crusher (Retsch SM 200). The experiment's setup is comparable to that which has been previously described elsewhere [27], as shown in Figure 1. The system consists of a quartz tube reactor fitted into a tubular furnace, a gas supply system coupled to a gas flow control meter, and a discharge gas bubbler connected at the reactor end. A boat (quartz) containing 1 g of the already-calcined catalyst sample was placed at the center of the reactor. The catalyst was reduced in situ under a 120 mL/min H$_2$/Ar gas atmosphere at 700 °C ramped at 20 °C/min for 30 minutes. Once the in-situ reduction was completed, the H$_2$/Ar gas mixture was disconnected, the gas flow was switched to Ar, and the flow rate was decreased to 100 mL/min. Then, 2 g of PP waste in a quartz boat was gently introduced into the reactor for deposition and subsequent nanomaterial formation for 30 minutes. The reactor and its components were then left to cool overnight in an environment of Ar. To guarantee that the experiment could be replicated and that the findings were reliable, the experiment was repeated three times, and the average value of the yield was noted. The yield of carbon deposition was calculated based on the mass difference between the fresh and spent catalysts with respect to the mass of waste PP feedstock used, as described by [28]. The experimental setup for the synthesis of CNTs from waste PP feedstock is shown in Figure 1.

The obtained black product was utilized of as-synthesised (pristine) nanomaterial which were individually purified using (1) air oxidation (2) chemical (acid treatment) oxidation, and (3) both chemical & air oxidation techniques, as outlined in the next section.

Purification of CNTs

Synthesized pristine CNTs were firstly pulverized using agate mortar and pestle into powder and were purified using three different purification protocols:

Air oxidation: In this method, 20 mg of the powdery pristine CNTs sample was subjected to thermal oxidation in air from room temperature to 450 °C at a ramp rate of 10 °C / min. and held for 4 hours using a tube furnace. The purified sample is labelled CNT-PA.

Acid oxidation treatment: 20 mg of pristine sample were refluxed in nitric acid for 24 hours at 80 °C and then filtered (over a 0.45 µm membrane). The filtered sample was hydrolyzed by ultrasonicating in DI water for 6 hours. Afterward, it was washed several times with DI water until the pH = 7. The sample was then dried at 80 °C in a vacuum oven for 24 hours. The purified sample was labelled CNT-PC.

Multi-step treatment (involving both acid oxidation and air (gas) oxidation: The pristine material was firstly oxidized in air and further treated in acid. About 20 mg of pristine sample was heated in air from room temperature to 450 °C and held for 4 hours. Thereafter, the air-oxidized sample was further refluxed in nitric acid for 24 hours at 80 °C, filtered, hydrolyzed, and ultrasonicated in DI water for 6 hours. The sample was further centrifuged and washed with DI water until the pH was neutral (pH= 7). The purified sample was dried at 80 °C in a vacuum oven for 24 hours and the sample was labelled as CNT-PAC.

The pristine CNTs, that is, the unpurified CNTs sample was labelled as CNT-P0. The pristine sample was hydrolyzed and sonicated in DI water for 6 hours and subsequently dried in a vacuum oven for 24 hours at 80 °C.

Characterization of Purified Nanostructure

The microstructure of purified nanomaterials was determined using a JEM-2100 transmission electron microscope (TEM) instrument (operated at an accelerated voltage of 200 k, with maximum resolution and magnification of 0.23 nm and 1500000x, respectively). A minute amount of the sample was sprinkled in ethanol and sonicated for 7 min; then few droplets of the mixture were carefully distributed onto a copper grid (carbon-coated), dried, and ready for image capture.

The degree of purity and defectiveness of purified and pristine nanomaterials were established using Raman Spectroscopy analysis using WITec focus innovations Raman spectrometer which was excited with the 632 nm laser line in the range of 500 to 3000 cm^{-1}.

The Thermogravimetric analysis (TGA) was conducted to evaluate the purity and the thermal stability of all purified and as-synthesized carbon products using the STA-7200RV HITACHI (Tokyo, Japan) thermal analyzer system from 100 to 900 °C in air.

The functional groups on the side walls and surfaces of purified and pristine nanomaterials were identified by Fourier Transform Infrared (FTIR) analysis using the KBr pellet technique on spectrum 100 FTIR spectrometer (Perkin-Elmer, Waltham, USA) scanned from 1000 to 4000 cm^{-1}.

X-ray diffraction patterns of all purified and as-prepared CNTs were obtained using a Rigaku Ultima 1V X-ray diffractometer (Czech Republic). Samples were X-rayed and recorded in the 2-theta range of 20–80 degrees with Cu Kα radiation, operating at 30 mA and 40 kV. The analysis of the data was carried out using PDXL (2.7.2.0) software.

RESULTS AND DISCUSSION

Effect of Purification Techniques on the Morphology of Plastic-Derived CNTs

Figure 2 depicts the TEM micrographs of pristine CNTs and all purified CNTs using different purification techniques. CNT-P0 consists of amass of amorphous carbon, and residual metal catalysts appearing as black particles inside and outside the walls and on the tips of as-produced CNTs. Also, the presence of other graphitic materials, such as nanofiber, could be observed. Chemical treatment with nitric acid resulted in the rupturing of the wall structure and shortening of the tubes, as shown in Figure 2C, and indicated with arrows at several points in the micrograph. However, it was effective in removing most of the metal nanoparticles. The air oxidation technique was able to remove most of the amorphous carbon impurities and more importantly, this protocol did not create sidewall defects or damage the CNTs' wall as indicated in Figure 2B. However, a large portion of metal nanoparticles were not adequately removed using the air oxidation technique. A similar observation was reported by Clancy et al. [21] during their investigation on air purification of SWCNTs.

Multi-step treatment involving both gas phase oxidation and chemical oxidation treatment, as shown in Figure 2D, also presented some degree of defects on the CNTs wall structure, but a majority of both amorphous carbon and metal nanoparticles were significantly removed using this

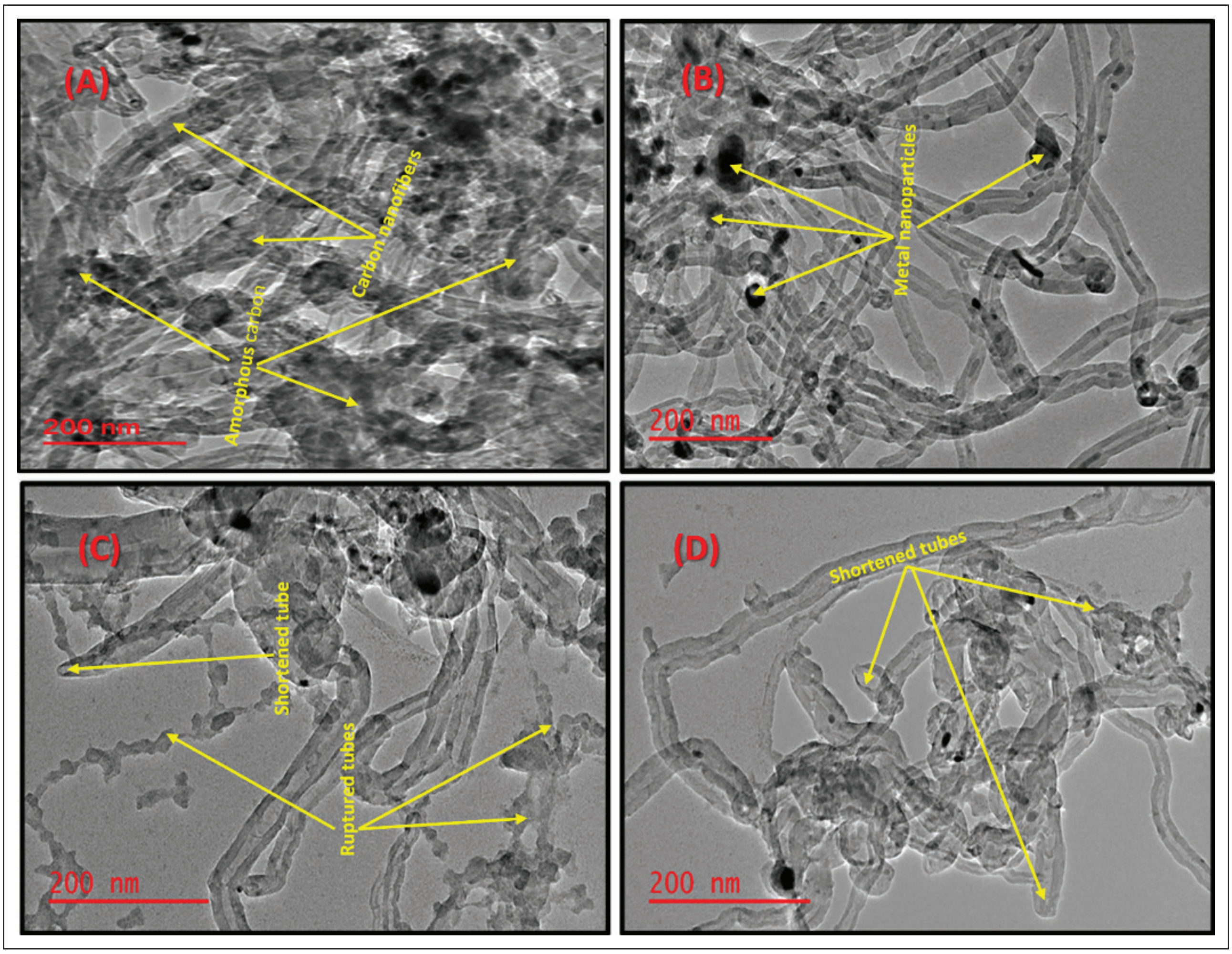

Figure 2. TEM micrographs of all purified and as-synthesized plastic waste-derived CNTs: **(A)** CNT-P0, **(B)** CNT-PA, **(C)** CNT-PC, and **(D)** CNT-PAC.

technique. Therefore, gas phase oxidation treatment (CNT-PA) resulted in less defective wall structure compared to the other two investigated techniques (both multi-step treatment and chemical oxidation treatment).

Effect of the Various Purification Methods on the Quality of Plastic Waste-Derived CNTs

Figure 3 shows the Raman spectra of all purified and pristine plastic waste-derived CNTs. A Raman spectroscopy study can be used to determine the crystallinity and degree of graphitization of CNTs [29, 30]. Therefore, the Raman spectra in Figure 3 depict three characteristic bands at 1345 cm^{-1}, 1574 cm^{-1}, and 2677 cm^{-1} identified as D, G, and G' (or 2D) bands, respectively. The D-band defines the disorder and defects in CNTs. The G-band is linked to the primary in-plane vibrations of $2p^2$ carbon atoms in graphene [31], while the G' (or 2D) band is related to the inter-valley two-phonon second-order Raman scattering process [32].

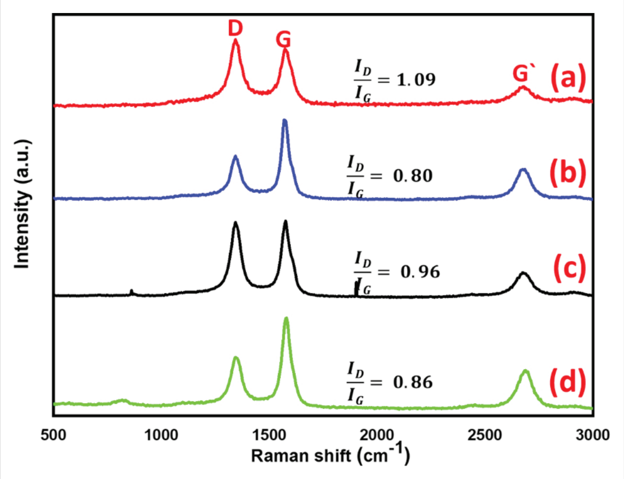

Figure 3. Raman spectra of pristine and all purified plastic waste-derived CNTs: **(a)** CNT-P0, **(b)** CNT-PA, **(c)** CNT-PC, and **(d)** CNT-PAC.

The peak intensity ratio of D to G (I_D/I_G) is considered to be proportional to the extent of disorder (graphitization) and purity of CNTs [33]. Therefore, a high I_D/I_G ratio signifies the presence of defects or disorders in the carbon lattice structure which means reduced crystallinity. The peak intensity ratio of G' to G ($I_{G'}/I_G$) is also indicative of the graphene content (graphitization) and stacking of the graphene layer. Amongst the investigated purification methods, CNT-PC showed the highest I_D/I_G ratio of 0.96 followed by CNT-

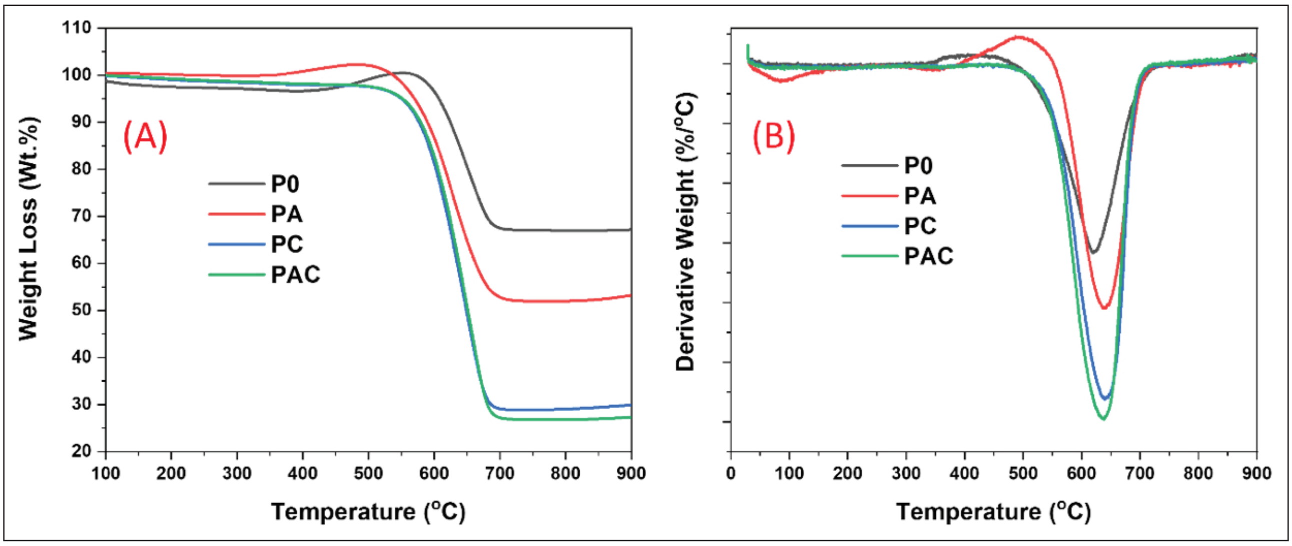

Figure 4. **(A)** TGA and **(B)** DTG thermographs of all purified and as-synthesized plastic waste-derived CNTs.

PAC and CNT-PA at 0.86 and 0.80, respectively. As shown in Figure 3, CNT-PA showed the least defect on the CNTs' walls compared to CNT-PC, which had the highest defect density. Therefore, the best quality CNTs were obtained in CNT-PA with the lowest I_D/I_G value. On the other hand, among the investigated purification protocols, the highest I_D/I_G value was obtained in CNT-PC indicating the lowest quality. The $I_{G'}/I_G$ ratio of CNT-PAC was 0.89 indicating the high graphitic structure which means that air and chemical oxidation were able to remove a considerable portion of impurities from the graphene layers. Therefore, CNT-PC presented the highest defective and disordered CNTs compared to the other treatment approaches investigated; this observation is in good agreement with the result obtained from the TEM analysis.

For the non-purified CNTs (CNT-P0), the D- band showed a larger and broader peak. Also, the weak G'-band peak is indicative of the presence of higher irregularities (reduced purity and quality) in the stacking of the graphene layers [34] which may be due to the presence of other impurities such as complex graphitic structures, amorphous carbon, and metal nanoparticles.

Figure 4 depicts the thermogravimetric curves of weight and derivative weight with respect to the oxidation temperature. Temperature-programmed oxidation (TPO) analysis provides salient information about the weight losses and thermal stability of purified and unpurified CNTs. The oxidation of carbon products in air into carbon dioxide results in the weight loss and is suggestive of the type and amount of carbon product present [35]. The catalyst mass losses were 70.1, 30.8, 48.2, and 72.3% for CNT-PC, CNT-P0, CNT-PA and CNT-PAC, respectively. The highest weight loss is associated with the highest carbon deposits [28]. Therefore, for all the purification protocols employed, CNT-PAC with the highest catalyst mass loss showed that almost all the catalyst nanoparticles were oxidized, indicating the highest quality. This finding is consistent with the Raman analysis result.

A higher oxidation temperature is linked to the higher graphitization degree of carbon products [36]. The oxidation peak of non-crystalline carbon, such as amorphous carbon, is reported to be at a lower temperature, usually between 350 and 400 °C, while crystalline filamentous carbon materials show a high-temperature peak above 500 °C [37]. For all purified nanomaterials, the oxidation peak was at 640 °C compared to the as-produced nanomaterial, which had an oxidation peak at 622 °C. Hence, all purified nanomaterials were more thermally stable than as-synthesized nanomaterials, suggesting a higher content of filamentous carbon.

The IR analysis is used to investigate the occurrence of functional groups (-OH, -C=O, -COOH, etc.) on the surfaces and sidewalls of the nanomaterials. The purification process usually results in the opening of end caps and cutting of nanotubes, with the corresponding attachment of functional groups [38, 39].

Figure 5 depicts the FTIR spectra showing the various surface functional groups present in all purified and as-synthesized plastic waste-derived CNTs. The peaks at 3707, 3742, 3779, and 3836 cm^{-1} are assigned to the stretching vibrations of the hydroxyl (-OH) group. Similarly, the well-defined peaks at 3450 cm^{-1} in Figure 5b and c are apportioned to the O-H band in C-OH [40] indicative of the stretching vibrations of hydroxyl (-OH) group arising from the oxidation on the sidewalls of CNTs. The bands at 2917 and 2920 cm^{-1} in Figure 5a and d are assigned to asymmetric stretching of C-H and C-O stretching vibrations, respectively. The peaks at 1580, 1590, 1634, and 1638 cm^{-1} are ascribed to the C=C stretching vibration which is indicative of the skeletal graphite structure of CNTs. Also, the peaks at 1383, 1387, 1389, and 1392 cm^{-1} are distinctive of the asymmetric/symmetric methyl stretching bands due to the deformation vibration of the C-H bond [41]. The peaks at 1210 and 1124 cm^{-1} in Figure 5c and d can be attributed to the C-H and C-O stretching mode which is associated with ether and epoxy groups arising from the oxidation of the nanotubes, which resulted in defective sidewalls, and band

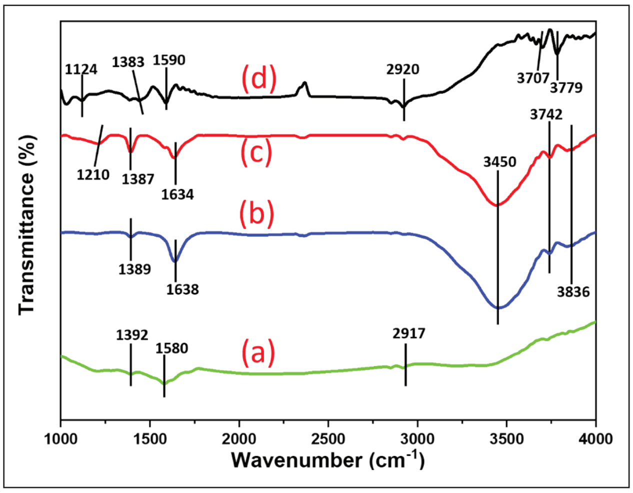

Figure 5. FTIR spectra of purified and pristine plastic waste-derived CNTs: **(a)** CNT-P0, **(b)** CNT-PA, **(c)** CNT-PC, and **(d)** CNT-PAC.

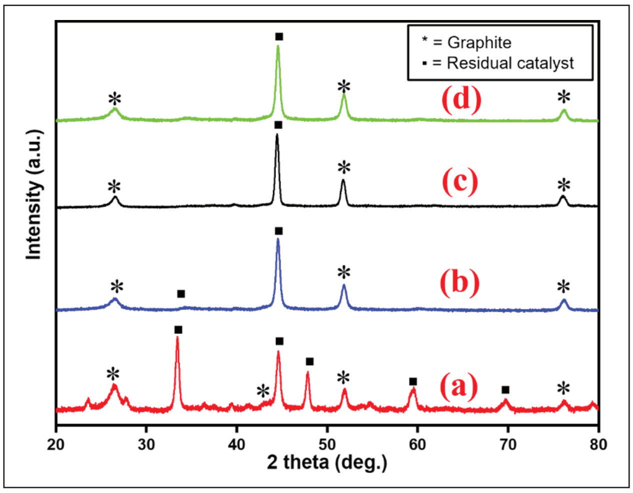

Figure 6. XRD patterns of as-synthesized and all purified plastic waste-derived CNTs: **(a)** CNT-P0, **(b)** CNT-PA, **(c)** CNT-PC, and **(d)** CNT-PAC.

overlapping, showing the extent of attack on the hexagonal carbon or the carbon-double bond at the sidewalls [42, 43]. This showed that hydroxyl (-OH) and carbonyl (-C=O) groups are introduced on the nanotube sidewall surfaces; a similar observation was reported by [40]. Therefore, both CNT-PAC and CNT-PC showed the attachment of more functional groups on the defective ends of the nanotubes. The purification protocol by acid oxidation and multi-step treatment resulted in nanotube functionalization.

The XRD patterns of pristine and all purified nanomaterials are shown in Figure 6. Diffraction peaks relating to graphite and residual metal catalysts were all labeled as shown. Characteristic graphite (CNTs) diffraction peaks related to (002), (004), and (110) planes which are linked to the atomic pair distribution function PDF 00-058-1638, were identified for all investigated purified and pristine nanomaterials.

The (002) diffraction plane also called Bragg peaks, is primarily used to describe the degree of alignment and distance between two graphene layers in the lattice [44, 45], and this diffraction peak appeared at 26.2° on the two-theta scale. For all purified CNTs, a d-spacing of 0.342 nm was obtained. The d-spacing of the crystalline carbon is evaluated using Bragg's equation $d = \lambda/2\sin\theta$ [46].

It could be observed that the (002) peak for CNT-P0 showed a slight broadening as compared to all purified CNTs, while the purification treatment under both thermal (air) and/or chemical oxidation techniques causes a reduction in the (002) peak intensity and interlayer spacing between the graphene sheets, confirming the removal of impurities since a decrease in the intensity of this peak depicts higher nanotube alignment [10]. This observation is similar to the result reported by Abdulrazzak and co-workers [47], where the presence of amorphous form of carbon resulted in an increased intensity and width of the (002) peak.

(002) and (004) peaks are employed to relate the interlayer distance within the graphene layers in the nanotube [47]. Another characteristic diffraction peak related to graphite (CNTs), which corresponds to the (100) plane, was detected in CNT-P0 at the two-theta position of 43.7°. This plane (100) describes the in-plane irregularity; according to Das et al. [48], the intensity of the (100) peak systematically decreases or disappears when all planes of the graphene sheets in the nanotubes are parallel to the (002) diffraction plane. Hence, it could be observed that the intensity of the (100) peak disappeared in all purified samples, suggesting that the intensity of this peak is sensitive to all the purification treatments and that all the planes in the purified CNTs are parallel to the Bragg peak. This elucidates that the treatment procedures undertaken treatment procedures impacted the nanotube's structures and graphitization. This observation correlates with the results obtained in TEM and Raman spectroscopy analyses.

The presence of other graphite (PDF 00-041-1487) and (PDF 00-056-0159) diffraction peaks were also detected in the XRD pattern of CNT-P0. The presence of arrays of diffraction peaks emanating chiefly from Ni metal catalyst impurities (PDF 00-004-0850) was identified in abundance in CNT-P0, followed by CNT-PA compared to other purified samples, this observation is in good agreement with the results obtained in the TEM, Raman, and TG analyses. Suggesting that acid oxidation and multi-step treatment approaches significantly removed practically all metal catalyst impurities from the synthesized samples.

CONCLUSION

The purification of plastic waste-derived CNTs was successfully carried out using three approaches: air-phase (gas) oxidation, liquid-phase (acid) oxidation, and multi-step oxidation. High-quality and pure CNTs can be obtained using the multi-step treatment method while taking advantage of combining the two protocols (both air and acid oxidation) which is also dependent on the intended application. From the results obtained from the XRD, Raman spectroscopy, and TEM analysis, it is shown that CNT-PC (acid/chemical treatment with nitric acid) presented the highest defects with significant structural and wall transformations, which may be due to the longer refluxing time. CNT-PAC presented the best graphitic structure and fewer defective CNTs compared to others, with an $I_{G'}/I_G$ value of 0.89 and ID/IG value of 0.86, while CNT-PA offered better structural and morphological CNTs and resulted in no loss in CNTs. Again, the chemically treated CNTs (CNT-PC) presented more structurally defective CNTs and shortened nanotubes with an ID/IG value of 0.96. CNT-PAC showed the highest weight loss of 72.3% indicating the highest quality and quantity of filamentous carbon present. Therefore, the structure and morphology of CNTs produced from plastic waste could be controlled by selecting suitable treatment conditions. However, it is recommended that shorter reflux time should be undertaken to minimize and control the possible damage to the CNTs wall structure when using the liquid-phase (acid treatment) approach.

ACKNOWLEDGEMENTS

The authors would like to acknowledge the support received from the University of Johannesburg (UJ), South Africa, under the Global Excellence Stature (GES) fellowship 4.0.

DATA AVAILABILITY STATEMENT

The authors confirm that the data that supports the findings of this study are available within the article. Raw data that support the finding of this study are available from the corresponding author, upon reasonable request.

CONFLICT OF INTEREST

The author declared no potential conflicts of interest with respect to the research, authorship, and/or publication of this article.

ETHICS

There are no ethical issues with the publication of this manuscript.

REFERENCES

[1] L. Yaqoob, T. Noor, and N. Iqbal, “Conversion of plastic waste to carbon-based compounds and application in energy storage devices,” ACS Omega, Vol. 7, pp. 13403–13435, 2022. [CrossRef]

[2] R. Rao, C.L. Pint, A.E. Islam, R.S. Weatherup, S. Hofmann, E.R. Meshot, F. Wu, C. Zhou, N. Dee, P.B. Amama, J. Carpena-Nuñez, W. Shi, D.L. Plata, E.S. Penev, B.I. Yakobson, P.B. Balbuena, C. Bichara, D.N. Futaba, S. Noda, H. Shin, K.S. Kim, B. Simard, F. Mirri, M. Pasquali, F. Fornasiero, E.I. Kauppinen, M. Arnold, B.A. Cola, P. Nikolaev, S. Arepalli, H. M. Cheng, D. N. Zakharov, E.A. Stach, J. Zhang, F. Wei, M. Terrones, D.B. Geohegan, B. Maruyama, S. Maruyama, Y. Li, W. W. Adams, and A. J. Hart, “Carbon nanotubes and related nanomaterials: Critical advances and challenges for synthesis toward mainstream commercial applications,” ACS Nano, Vol. 12, pp. 11756–11784, 2018. [CrossRef]

[3] A. Eatemadi, H. Daraee, H. Karimkhanloo, M. Kouhi, N. Zarghami, A. Akbarzadeh, M. Abasi, Y. Hanifehpour, and S. W. Joo, “Carbon nanotubes: properties, synthesis, purification, and medical applications,” Nanoscale Research Letters, Vol. 9, Article 393, 2014. [CrossRef]

[4] C.E.M. Oliveira, E.E. da Silva, E.A. de Morals, V. Geraldo, “Carbon nanotubes research developments: Published scientific documents and patents, synthesis, and production,” in: J. Abraham, S. Thomas, N. Kalarikkal (Eds.), Handb. Carbon Nanotub., Springer Nature Switzerland AG, Cham, Switzerland, pp. 1937–1974, 2022. [CrossRef]

[5] S. Temizel-Sekeryan, F. Wu, and A. L. Hicks, “Global scale life cycle environmental impacts of single- and multi-walled carbon nanotube synthesis processes,” International Journal of Life Cycle Assessment, Vol. 26, pp. 656–672, 2021. [CrossRef]

[6] B.O. Murjani, P. S. Kadu, M. Bansod, S. S. Vaidya, and M. D. Yadav, “Carbon nanotubes in biomedical applications: current status, promises, and challenges,” Carbon Letters, Vol. 32, pp. 1207–1226, 2022. [CrossRef]

[7] H. U. Modekwe, O. O. Ayeleru, M. A. Onu, T. T. Nyam, M. A. Mamo, K. Moothi, M. O. Daramola, and P. A. Olubambi, “The current market for carbon nanotube materials and products,” in: J. Abraham, S. Thomas, N. Kalarikkal (Eds.), Handb. Carbon Nanotub., Springer Nature Switzerland AG, Cham, Switzerland, pp. 619–633, 2022. [CrossRef]

[8] E. Inshakova, A. Inshakova, and A. Goncharov, “Engineered nanomaterials for energy sector: Market trends, modern applications and future prospects,” IOP Conference Series: Materials Science and Engineering, Vol. 971, Article 032031, 2021. [CrossRef]

[9] U.P.M. Ashik, W.M.A.W. Daud, and J. Hayashi, “A review on methane transformation to hydrogen and nanocarbon: Relevance of catalyst characteristics and experimental parameters on yield,” Renew. Sustain. Energy Review, Vol. 76, pp. 743–767, 2017. [CrossRef]

[10] R. Das, M. E. Ali, S.B. Abd Hamid, M.S.M. Annuar, and S. Ramakrishna, “Common wet chemical agents for purifying multiwalled carbon nanotubes,” Journal of Nanomaterials, Vol. 2014, pp. 237, 2015. [CrossRef]

[11] X. Jia, and F. Wei, “Advances in production and applications of carbon nanotubes,” Topics in Current Chemistry, Vol. 375, Article 18, 2017. [CrossRef]

[12] H. U. Modekwe, M. A. Mamo, K. Moothi, and M. O. Daramola, “Effect of different catalyst supports on the quality, yield and morphology of carbon nanotubes produced from waste polypropylene plastics,” Catalysts, Vol. 11, Article 692, 2021. [CrossRef]

[13] A. F. Ismail, P. S. Goh, J. C. Tee, S. M. Sanip, and M. Aziz, “A review of purification techniques for carbon nanotubes,” Nano Reports Reviews, Vol. 3, pp. 127–143, 2008. [CrossRef]

[14] P. Pandey, M. Dhiman, A. Kansal, and S. P. Subudhi, "Plastic waste management for sustainable environment: techniques and approaches," aste Disposal & Sustainable Energy, Vol. 5, pp. 205–222, 2023. [CrossRef]

[15] PlasticsEurope, "Plastics-the Facts 2019. An analysis of European plastics production, demand and waste data," Belgium, 2019.

[16] R. Geyer, J. R. Jambeck, and K. L. Law, "Production, use, and fate of all plastics ever made," Science Advances, Vol. 3, pp. 25–29, 2017. [CrossRef]

[17] K.L. Law, "Plastics in the marine environment," Annual Review of Marine Science, Vol. 9, pp. 205–229, 2017. [CrossRef]

[18] P.-X. Hou, C. Liu, and H.-M. Cheng, "Purification of carbon nanotubes," Carbon, Col. 46, pp. 2003–2025, 2008. [CrossRef]

[19] P. Mahalingam, B. Parasuram, T. Maiyalagan, and S. Sundaram, "Chemical methods for purification of carbon nanotubes- A Review," Journal of Environmental Nanotechnology, Vol. 1, pp. 53–61, 2012.

[20] S. Boncel, and K. K. K. Koziol, "Enhanced graphitization of c-CVD grown multi-wall carbon nanotube arrays assisted by removal of encapsulated iron-based phases under thermal treatment in argon," Applied Surface Science, Vol. 301, pp. 488–491, 2014. [CrossRef]

[21] A. J. Clancy, E. R. White, H. H. Tay, H. C. Yau, and M. S. P. Shaffer, "Systematic comparison of conventional and reductive single-walled carbon nanotube purifications," Carbon, Vol. 108, pp. 423–432, 2016. [CrossRef]

[22] A. H. Hammadi, A. M. Jasim, F. H. Abdulrazzak, A. M. A. Al-Sammarraie, Y. Cherifi, R. Boukherroub, F. H. Hussein, "Purification for carbon nanotubes synthesized by flame fragments deposition via hydrogen peroxide and acetone," Materials (Basel), Vol. 13, Article 2342, 2020. [CrossRef]

[23] I. Pelech, U. Narkiewicz, A. Kaczmarek, A. Jedrzejewska, "Preparation and characterization of multi-walled carbon nanotubes grown on transition metal catalysts," Polish Journal of Chemical Technology, Vol. 16, pp. 117–122, 2014. [CrossRef]

[24] J. C. Goak, S. H. Lee, and N. Lee, "Effect of purification on the electrical properties of transparent conductive films fabricated from single-walled carbon nanotubes," Diamond and Related Materials, Vol. 106, Article 107815, 2020. [CrossRef]

[25] A. Ahamed, A. Veksha, K. Yin, P. Weerachanchai, A. Giannis, and G. Lisak, "Environmental impact assessment of converting flexible packaging plastic waste to pyrolysis oil and multi-walled carbon nanotubes," Journal of Hazardous Materials, Vol. 390, Article 121449, 2020. [CrossRef]

[26] H. U. Modekwe, M. A. Mamo, M. O. Daramola, and K. Moothi, "Catalytic performance of calcium titanate for catalytic decomposition of waste polypropylene to carbon nanotubes in a single-stage CVD reactor," Catalysts, Vol. 10, Article 1030, 2020. [CrossRef]

[27] H. U. Modekwe, M. Mamo, K. Moothi, and M. O. Daramola, "Synthesis of bimetallic NiMo/MgO catalyst for catalytic conversion of waste plastics (polypropylene) to carbon nanotubes (CNTs) via chemical vapour deposition method," Materials Today: Proceedings, Vol. 38, pp. 549–552, 2021. [CrossRef]

[28] D. Yao, and C. H. Wang, "Pyrolysis and in-line catalytic decomposition of polypropylene to carbon nanomaterials and hydrogen over Fe- and Ni-based catalysts," Applied Energy, Vol. 265, Article 114819, 2020. [CrossRef]

[29] M. Flygare, and K. Svensson, "Quantifying crystallinity in carbon nanotubes and its influence on mechanical behaviour," Materials Today Communications, Vol. 18, pp. 39–45, 2019.

[30] A. Jorio, and R. Saito, "Raman spectroscopy for carbon nanotube applications," Journal of Applied Physics, Vol. 129, Article 021102, 2021. [CrossRef]

[31] D. Yao, H. Yang, H. Chen, and P. T. Williams, "Co-precipitation, impregnation and so-gel preparation of Ni catalysts for pyrolysis-catalytic steam reforming of waste plastics," Applied Catalysis B: Environmental, Vol. 239, pp. 565–577, 2018. [CrossRef]

[32] M. S. Dresselhaus, G. Dresselhaus, R. Saito, and A. Jorio, "Raman spectroscopy of carbon nanotubes," Physics Reports, Vol. 409, pp. 47–99, 2005. [CrossRef]

[33] A. A. Aboul-Enein, and A. E. Awadallah, "Impact of Co/Mo ratio on the activity of CoMo/MgO catalyst for production of high-quality multi-walled carbon nanotubes from polyethylene waste," Materials Chemistry and Physics, Vol. 238, Article 121879, 2019. [CrossRef]

[34] E. C. Igbokwe, M. O. Daramola, and S. E. Iyuke, "Production of carbon nanotube yarns via floating catalyst chemical vapor deposition: Effect of synthesis temperature on electrical conductivity," Results in Physics, Vol. 15, Article 102705, 2019. [CrossRef]

[35] J. Jia, A. Veksha, T. Lim, and G. Lisak, "In situ grown metallic nickel from X-Ni (X= La , Mg , Sr) oxides for converting plastics into carbon nanotubes: Influence of metal support interaction," Journal of Cleaner Produvtion, Vol. 258, pp. 1–11, 2020. [CrossRef]

[36] J. C. Acomb, C. Wu, and P. T. Williams, "The use of different metal catalysts for the simultaneous production of carbon nanotubes and hydrogen from pyrolysis of plastic feedstocks," Applied Catalysis B: Environmenta, Vol. 180, pp. 497–510, 2016. [CrossRef]

[37] A. A. Aboul-Enein, and A. E. Awadallah, "Production of nanostructure carbon materials via non-oxidative thermal degradation of real polypropylene waste plastic using La2O3 supported Ni and Ni–Cu catalysts," Polymer Degradation and Stability, Vol. 167, pp. 157–169, 2019. [CrossRef]

[38] A. B. Makama, A. Salmiaton, N. Abdullah, T. S. Y. Choong, and E. B. Saion, "Recent developments in purification of single wall carbon nanotubes," Separation Science and Technology, Vol. 49, pp. 2797–2812, 2014. [CrossRef]

[39] P. De Luca, C. Siciliano, A. Macario, and J. B. Nagy, "The role of carbon nanotube pretreatments in the adsorption of benzoic acid," Materials (Basel), Vol. 14, Article 2118, 2021. [CrossRef]

[40] E. M. Elsehly, N. G. Chechenin, A. V. Makunin, H. A. Motaweh, E. A. Vorobyeva, K. A. Bukunov, E. G. Leksina, and A. B. Priselkova, "Characterization of functionalized multiwalled carbon nanotubes and application as an effective filter for heavy metal removal from aqueous solutions," The Chinese Journal of Chemical Engineering, Vol. 24, pp. 1695–1702, 2016. [CrossRef]

[41] H. Hu, T. Zhang, S. Yuan, and S. Tang, "Functionalization of multi-walled carbon nanotubes with phenylenediamine for enhanced CO2 adsorption," Adsorption, Vol. 23, pp. 73–85, 2017. [CrossRef]

[42] H. U. Modekwe, M. Mamo, K. Moothi, and M. O. Daramola, "Polypropylene waste-derived carbon nanotubes (CNTs) via single-stage CVD technique: Determination of crystallinityIOP Conference Series: Materials Science and Engineering, Vol. 1107, Article 012067, 2021. [CrossRef]

[43] R. Yudianti, H. Onggo, Sudirman, Y. Saito, T. Iwata, and J. Azuma, "Analysis of functional group sited on multiwall carbon nanotube surface," The Open Materials Science Journal, Vol. 5, pp. 242–247, 2011. [CrossRef]

[44] A. Cao, C. Xu, J. Liang, D. Wu, and B. Wei, "X-ray diffraction characterization on the alignment degree of carbon nanotubes," Chemical Physics Letters, Vol. 344, pp. 13–17, 2001. [CrossRef]

[45] D. K. Singh, P. K. Iyer, and P. K. Giri, "Diameter dependence of interwall separation and strain in multiwalled carbon nanotubes probed by X-ray diffraction and Raman scattering studies," Diamond and Related Materials, Vol. 19, pp. 1281–1288, 2010. [CrossRef]

[46] D. Yao, H. Yang, Q. Hu, Y. Chen, H. Chen, and P. T. Williams, "Carbon nanotubes from post-consumer waste plastics: Investigations into catalyst metal and support material characteristics," Applied Catalysis B: Environmental, Vol. 280, Article 119413, 2021. [CrossRef]

[47] F. H. Abdulrazzak, A. F. Alkaim, F. H. Hussein, "Behavior of X-Ray analysis of carbon nanotubes," in Perspect. Carbon Nanotub., IntechOpen, London, United Kingdom, 2019. [CrossRef]

[48] R. Das, S. B. A. Hamid, M. E. Ali, S. Ramakrishna, and W. Yongzhi, "Carbon nanotubes characterization by X-ray powder diffraction – A Review," Current Nanoscience, Vol. 11, pp. 1–13, 2015. [CrossRef]